Anthropic disturbances impact the soil microbial network structure and stability to a greater extent than natural disturbances in an arid ecosystem

Kenji Maurice, Amélia Bourceret, Sami Youssef, Stéphane Boivin, Liam Laurent-Webb, Coraline Damasio, Hassan Boukcim, Marc-André Selosse, Marc Ducousso

Science of the Total Environment 907 (2024) 167969

Contents lists available at ScienceDirect

Science of the Total Environment

journal homepage: www.elsevier.com/locate/scitotenv

Anthropic disturbances impact the soil microbial network structure and stability to a greater extent than natural disturbances in an arid ecosystem

Kenji Maurice [a,*], Amélia Bourceret [b], Sami Youssef [c], Stéphane Boivin [a], Liam Laurent-Webb [b], Coraline Damasio [a], Hassan Boukcim [c,d], Marc-André Selosse [b,e,f], Marc Ducousso [a]

[a] LSTM, Univ Montpellier, CIRAD, INRAE, IRD, SupAgro, UMR082 LSTM, 34398 Montpellier Cedex 5, France
[b] ISYEB, Muséum national d'Histoire naturelle, CNRS, EPHE-PSL, Sorbonne Université, 57 rue Cuvier, CP39, 75005 Paris, France
[c] Department of Research and Development, VALORHIZ, 1900, Boulevard de la Lironde, PSIII, Parc Scientifique Agropolis, F34980 Montferrier sur Lez, France
[d] ASARI, Mohammed VI Polytechnic University, Lot 660, Hay Moulay Rachid Ben Guerir, 43150, Morocco
[e] Department of Plant Taxonomy and Nature Conservation, University of Gdańsk, ul. Wita Stwosza 59, 80-308 Gdańsk, Poland
[f] Institut Universitaire de France, Paris, France

HIGHLIGHTS

- Diversity was insufficient to assess microbial response to environmental stress.
- Rhizosphere networks differed between long- and short-termed disturbances.
- Short-termed anthropic disturbances resulted in the lower network stability.
- Natural environments and long termed disturbances favor network stability.
- Fungi improved the crossdomain networks stability in the long-termed disturbance.

GRAPHICAL ABSTRACT

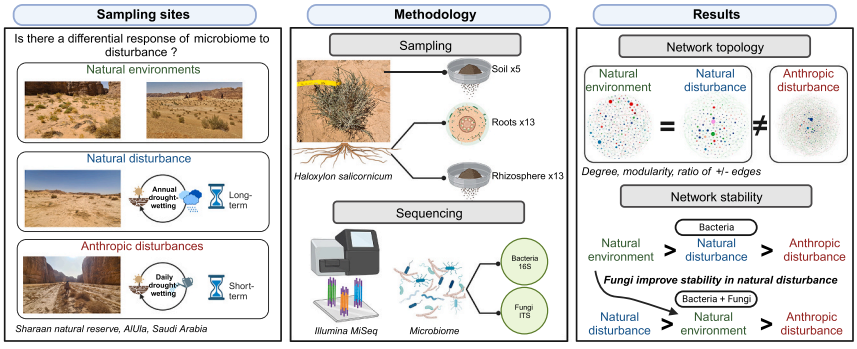

ARTICLE INFO

Editor: Abasiofiok Mark Ibekwe

Keywords:
Soil microbiome
Co-occurrence network
Stability
Disturbance

ABSTRACT

Growing pressure from climate change and agricultural land use is destabilizing soil microbial community interactions. Yet little is known about microbial community resistance and adaptation to disturbances over time. This hampers our ability to determine the recovery latency of microbial interactions after disturbances, with fundamental implications for ecosystem functioning and conservation measures. Here we examined the response of bacterial and fungal community networks in the rhizosphere of *Haloxylon salicornicum* (Moq.) Bunge ex Boiss. over the course of soil disturbances resulting from a history of different hydric constraints involving flooding-drought successions. An anthropic disturbance related to past agricultural use, with frequent successions of flooding and drought, was compared to a natural disturbance, i.e., an evaporation basin, with yearly flooding-drought successions. The anthropic disturbance resulted in a specific microbial network topology characterized by lower modularity and stability, reflecting the legacy of past agricultural use on soil microbiome. In contrast, the natural disturbance resulted in a network topology and stability close to those of natural environments despite the lower alpha diversity, and a different community composition compared to that of the other

* Corresponding author.
E-mail address: kenji.maurice@gmail.com (K. Maurice).

https://doi.org/10.1016/j.scitotenv.2023.167969
Received 16 August 2023; Received in revised form 16 October 2023; Accepted 18 October 2023
Available online 30 October 2023

sites. These results highlighted the temporality in the response of the microbial community structure to disturbance, where long-term adaptation to flooding-drought successions lead to a higher stability than disturbances occurring over a shorter timescale.

1. Introduction

Soil microorganisms play crucial roles in ecosystem functioning (e.g. C and N recycling) (Kuypers et al., 2018) and are the foundation of higher trophic strata (e.g. plants, animals). These organisms are of major interest for maintaining ecosystem stability (Bardgett and van der Putten, 2014; Kuypers et al., 2018), as they interact with each other (through intra- and inter-kingdom interactions) and with plants (Hassani et al., 2018; Trivedi et al., 2020), thereby improving their establishment and survival, while modulating their tolerance and resistance to environmental pressures (Berendsen et al., 2012; Hubbard et al., 2019; Liu et al., 2018). Increasing environmental pressures, direct consequences of human activities (e.g. agricultural activities, C emissions) or indirectly (e.g. climate change, desertification) have profound impacts on soil microbial communities worldwide (Cavicchioli et al., 2019; Jansson and Hofmockel, 2020; Yuan et al., 2021). Soil microbe-microbe interactions are sensitive to variations caused by environmental pressures or stresses, such as erosion (Qiu et al., 2021), climate warming (Yuan et al., 2021) or land use (de Vries et al., 2012). These stresses affect overall microbial community stability, resistance and resilience to future extreme events, such as drought (de Vries et al., 2018; Delgado-Baquerizo et al., 2020), and hamper the myriad ecosystem services they provide (e.g. C and N cycling) through the extinction of belowground microbial interactions (Malik et al., 2018; Viruel et al., 2022; Wagg et al., 2019).

In recent years, an analytical framework based on co-occurrence networks has emerged for studying microbial associations and their stability (Barberán et al., 2012; Berry and Widder, 2014; Coyte et al., 2015). Co-occurrence networks are built using graph theory tools, and their structure and topology provide information on associations between microbial taxa, thereby facilitating assessment of the resistance (i.e., how a community remains unchanged during a disturbance) and resilience (i.e., how a community returns to its initial state after a disturbance) of microbial communities coping with environmental stress. Although they do not support biotic interactions (Peterson et al., 2020) and care must be taken for both their construction and interpretation (Goberna and Verdú, 2022; Hirano and Takemoto, 2019; Röttjers and Faust, 2018), networks provide a useful framework for microbiome structure analysis, especially for the study of microbiome responses along stress gradients and land use types (Karimi et al., 2019, 2017). For instance, Banerjee et al. (2019) observed a decrease in network complexity (e.g. betweenness, assortativity, cohesion) and in abundance of keystone taxa in conventional agricultural systems as compared to organic systems. Decreased network complexity has also been observed across soil erosion gradients (Qiu et al., 2021) and in secondary successions following anthropic disturbance (Yu et al., 2022). Furthermore, modifications in microbial associations such as increased positive associations have been observed in an elevation stress gradient of water and nutrient availability (Hernandez et al., 2021). However, little is known on the systematic links between environmental stresses and microbial interaction stability. In particular, it has yet to be determined whether increased stress invariably has a negative impact on community stability (Hernandez et al., 2021). One aspect of this issue has received little attention, i.e., the extent to which disturbances have a legacy effect on microbial associations. Assessing (i) whether long-term stresses influence the stability of soil microbial communities to the same extent as short-term stresses and, if so, (ii) whether there is a disturbance legacy on community resilience and/or resistance, is essential to gain insight into how future climatic events and land use changes could affect microbial interactions.

Here, in a desertic ecosystem, we aimed to investigate the effect of stresses (natural and anthropic) occurring on various time scales on microbial community diversity, composition and interactions. Using natural environments as reference, we hence compared the legacy effects of anthropic and natural disturbances, both subjected to hydric constraints, on microbial diversity and network structure and stability. We focused on an old date palm farm abandoned 15 years prior to the study after 10 years of cultivation with a flood irrigation system, resulting in ongoing soil induration, as an anthropic disturbance. We compared it to an evaporation basin, i.e., a topologically induced microecosystem subject to a natural disturbance involving a succession of annual floods and droughts that had occurred over a period of several hundred years. We hypothesized that: (i) microbial diversity would be impacted by disturbances compared to the natural ecosystem, (ii) the microbial network topology (e.g., degree, betweenness, centrality and modularity) would differentiate natural and disturbed sites, and (iii) stability would be lower in the disturbed sites.

2. Material and methods

2.1. Sampling site

The five sampling sites were located in the Sharaan Nature Reserve in AlUla (Medina Province, Saudi Arabia). Three of them were representative of soil disturbances resulting from wetting-dessication successions: (i) from past agricultural uses, where flood irrigation was practised daily over the 10 year agricultural usage period before being abandoned 15 years prior to the study (OF), (ii) natural recovery from past agricultural usage with the same practices as OF, where plants recolonized the ecosystem (LR), and (iii) an evaporation basin (EB), i.e., a topological depression with yearly wetting-dessication successions due to scarce rain events which we considered to be a natural disturbance. These sites were compared to two natural undisturbed areas without any significant anthropic activities (Nat 1, Nat 2) (Fig. A1, A2). At each of the 5 sites, 5 bare soil samples and 13 root and rhizospheric soil samples under *Haloxylon salicornicum salicornicum* (Moq.) Bunge ex Boiss. plants, i.e., a stress tolerant Amaranthaceae species widespread in desert areas, were collected. Rhizospheric soil, in the close vicinity of roots was sampled with sterile equipment. All soil samples were sieved to 2 mm and root samples were stored in a 2 % CTAB solution at 4 °C until molecular analysis. For each sampling point, qualitative variables describing the soil cover were measured.

2.2. Soil chemical composition and pH

The relative abundance of soil chemical elements (from magnesium to uranium) was measured by X-ray fluorescence (XRF). Triplicate soil samples were pressed at 20 t for 2 min with 1:3 v:v of SpectroBlend® (SCP Science, Baie-D'Urfé, Québec, Canada). Each pellet was then analyzed in triplicate with an XRF S1 Titan analyzer (Bruker, Billerica, Massachusetts, USA) using the 'geoexploration' parameter with a total exposure time of 105 s (Supplementary file 1). The nine measurements were then averaged and calibrated according to the limit of optical detection (LOD) of each analyzed element (provided by Brucker). A pH meter (pH Meter Knick 766, Knick international, Berlin, Germany) was used to assess pH H_2O and pH KCl in a 1:5 v:v of H_2O or KCl (1 mol.L^{-1}).

2.3. DNA extraction

To ensure high DNA concentrations, soil DNA extractions were

performed after shaking 5 mL of soil in 20 mL of sterile milliQ water. The supernatant was centrifugated for 5 min at 12,000 g and the pellet was isolated for extraction (Högfors-Rönnholm et al., 2018). Roots were washed with sterile water, flash frozen with liquid nitrogen and ground with a ceramic ball for 3 cycles of 30 s at 5.0 speed in a FastPrep-24™ 5G instrument from MP Biomedicals™ (Irvine, California, USA). Extractions were then performed with the FastDNA Spin kit for soil (MP Biomedicals™). DNA concentrations were measured by fluorescence with a Quant-iT™ PicoGreen™ dsDNA Assay Kit (ThermoFisher Scientific™, Waltham, Massachusetts, USA) using a Tecan Spark ® (Tecan Group Ltd., Männedorf, Switzerland). The concentration measurement was used to normalize the DNA concentrations to 0.3 ng.µL-1 before PCR amplification.

2.4. PCR conditions

The hypervariable V3-V4 region of the 16S rRNA gene was amplified using 479F (5′ CAGCMGCYGCNGTAANAC 3′) and R888 (5′ CCGYCAATTCMTTTRAGT 3′) primers (Terrat et al., 2015). ITS86F (5′ GTGAATCATCGAATCTTTGAA 3′) and ITS4 (5′ TCCTCCGCTTATTGATATGC 3′) primers were used to amplify the fungal ITS2 (Op De Beeck et al., 2014). Reactions were performed in 20 µL and consisted of 10 µL of Buffer Master mix containing Thermo Scientific Phusion™ High-Fidelity DNA Polymerase (ThermoFisher Scientific™), 0.5 µL of DMSO, 4.5 µL of DNAse free water, 3 µL of DNA (0.3 ng.µL^{-1}), 1 µL of forward primer and 1 µL of reverse primer tagged with a short nucleotide sequence. The PCR conditions used were identical for the fungal and bacterial amplifications and were performed in a Veriti 96-well Thermal Cycler (ThermoFisher Scientific™) under the following conditions: 10 min initial denaturation, 35 cycles each including denaturation at 94 °C for 10 s, annealing at 55 °C for 20 s, and extension at 72 °C for 20 s, with a final polymerization extension at 72 °C for 7 min. All reactions were performed in triplicate and then pooled before deposition on 2 % agarose gel, with the corresponding negative control, for amplification quality control.

2.5. Purification of PCR products and preparation of sequencing libraries

ITS2 region amplification products were purified using Agencourt AMPure XP beads (Beckman Coulter Inc., Fullerton, California, USA) and performed on a magnetic rack with a 1:1 (v:v) ratio of AMPure XP per PCR product. The magnetic beads were then rinsed twice with 70 % ethanol before final elution in 70 µL of Qiagen EB buffer. For 16S purification, an additional PCR product migration step on 2 % agarose gel (80 V, 90 min) was performed to separate and recover the band specific to bacterial 16S (lower band, around 400 bp), and eliminate plant chloroplastic 16S DNA (higher band, >600 bp, co-amplified during PCR). The recovered bands were purified using the QIAquick gel purification kit (Qiagen, Hilden, Germany). The purified PCR product concentration was then measured with PicoGreen and one equimolar pool (50 ng/sample) for each marker gene (16S and ITS2) was prepared. Each pool was finally purified twice using Agencourt AMPure XP beads, quantified and finally eluted in 40 µL of EB buffer (Qiagen).

2.6. Illumina MiSeq sequencing and data processing

MetaFast library preparation and amplicon sequencing were performed on an Illumina 2 × 250 bp MiSeq platform by Fasteris SA, Switzerland (www.fasteris.com). We used a pipeline based on VSEARCH (Rognes et al., 2016) and available in GitHub (https://github.com/BPerezLamarque/Scripts/) for data processing (Perez-Lamarque et al., 2022; Petrolli et al., 2021). Briefly, paired-end reads were merged using the fastq_mergepairs function with default parameters. We applied a quality check and removed merged reads with more than two alignment errors. Then filtered merged reads were assigned to the respective samples based on tagged primers (demultiplexing) with 0 accepted error regarding the primers and tag sequences using the Cutadapt tool (Martin, 2011). We removed chimeras de novo by using the VSEARCH uchime3_denovo option and assigned the taxonomy to each amplicon sequence variant (ASV) using the usearch_global option with default parameters. We used SILVA 138.1 and UNITE (v.8.0) databases for bacteria and fungi, respectively (Kõljalg et al., 2020; Quast et al., 2012). The ASV tables were then filtered from contaminants based on comparisons with amplified negative controls using the DECONTAM (prevalence method) R package (Davis et al., 2018). Only ASVs with long sequences (>200 bp), assigned to the bacterial and fungal kingdom, presenting an acceptable abundance (≥ 10 reads) and amplified in at least one sample, were kept for subsequent analyses.

2.7. Compositional analysis of X-ray fluorescence soil atomic elements

As with sequencing data, XRF data are proportions, in relative abundance, and are therefore enclosed in a compositional space (a simplex), where Euclidean distances are not meaningful (Aitchison, 1981). Centered log ratio transformation was applied to map data into a real space where Euclidean distances could be used for dimensionality reduction and visualized using principal component analysis according to sites. Only main elements, i.e., Mg, Al, Si, P, K, Ca, Ti, Mn and Fe, were retained as variables. Cumulative probability distribution curves were plotted to determine the proportional enrichment of each microelement between natural and disturbed environments, as recommended by Reimann et al. (2012).

2.8. Microbial alpha and beta diversity analysis

ASV tables were Hellinger transformed and then a Bray-Curtis distance matrix was used to compute differences in microbial community composition per site (Nat 1, Nat 2, OF, LR, EB) and compartment (rhizosphere and root) and visualized using non-metric multidimensional scaling (nMDS). Permutational analysis of variance (PERMANOVA) was then performed to test microbial community differences over sites and compartments and the interaction of these two parameters (Supplementary file 2). Samples with <5000 reads were discarded, then alpha diversity indexes (Chao1: abundance-based richness, and Shannon: richness estimator that takes evenness into account) were computed per amplicon on rarefied ASVs tables at 5000 reads. Wilcoxon tests were then applied to test paired differences over sites for each rhizospheric and root microbial community. As rarefaction can introduce sequencing data bias (McMurdie and Holmes, 2014), we addressed this potential issue using a combined strategy to assess the effect of sequencing depth on sampling completeness and on the dispersion induced on diversity estimation. First, we performed bootstraps on rarefaction curves to observe ASV counts by increasing the library size to see if a plateau was reached (Fig. A3). Then, using the Mirlyn package (Cameron et al., 2021) we performed stepwise bootstraps on read numbers per sample to assess Shannon diversity index value changes by increasing sequencing depth (Fig. A4). Finally, in each individual sample we tested the dispersion induced by the rarefaction process at different sequencing depth (Fig. A4). All of these elements were used to determine the rarefaction level.

2.9. Network construction

Before network construction, we subsetted new ASV tables from the original dataset for each sampling site (Nat 1, Nat 2, OF, LR, EB) and compartment (rhizosphere and root) to avoid confusing environmental filtering effects. We used rhizosphere samples for network construction as the soil-plant root interface is known to be the most responsive to environmental changes compared to roots (Shi et al., 2016) we also noted this feature in our dataset. Rare taxa were eliminated (<10 reads across samples) and prevalence thresholds of 20 % for 16S and 15 % for ITS were used. Networks were constructed using SPIEC-EASI (Kurtz

et al., 2015), which is robust against compositional data by using clr-transformation to remove the unit-sum constraint of compositional data, as proposed by Aitchison (Aitchison, 1981). LASSO regularization and cross-validation were performed internally using SPIEC-EASI to detect the most parsimonious network structure by inverse covariance estimation along a lambda path (λ = sparsity). Each network was constructed with a lambda ratio of 0.01, with 50 lambda values over 999 cross-validations, while neighborhood selection was performed using the Meinshausen and Bühlmann method ('mb'). Models were selected using the Stability Approach to Regularization Selection (StARS) algorithm with a stability threshold of 0.05, that was assessed for each network construction ($n = 11$, 10, 10, 9 and 11 samples for Nat 1, Nat 2, OF, EB and LR, respectively). Cross-domain interaction networks with bacteria and fungi for each site and compartment were constructed using the extended SPIEC-EASI method (Tipton et al., 2018).

2.10. Network structural properties

Node degree (i.e., the number of connections to other nodes), betweenness centrality (i.e., a centrality measure based on the shortest path between nodes), average path length (i.e., a robust measure of network topology defined as the average number of steps along the shortest paths for all possible pairs of network nodes), and positive-to-negative edge ratio were calculated with igraph (Csardi and Nepusz, 2006) and Gephi 0.10 (Interactions proportion at the phylum level is available in Supplementary files 3–4). As networks size in both nodes and edges number are different, degree was normalized by dividing the node degree of each network by n-1, where n is the number of nodes. Betweenness centrality was normalized using the formula from igraph: $B^n = \frac{2B}{(n-1)(n-2)}$ where B^n is the normalized betweenness, B is the absolute betweenness and n is the number of nodes. Modularity was computed using the algorithm of Blondel et al. (2008) with the formula of Newman (2004) for weighted networks:

$$Q = \frac{1}{2m}\sum_{i,j}\left[A_{ij} - \frac{k_i k_j}{2m}\right]\delta(c_i, c_j),$$

where A_{ij} is the weight of the edge between i and j, $k_i = \sum_j A_{ij}$ is the sum of weights of the edges attached to vertex i, c_i is the community to which vertex i is attached, $m = \frac{1}{2}\sum_{ij} A_{ij}$, the δ-function $\delta(u, v)$ is 1 if $u = v$, which reflects the fact that they are in the same module, and 0 otherwise. Q values close to 1 mean that there is a higher proportion of within- than between-module edges. To assess changes in network centrality across sites, we assessed the distribution and then performed Tukey HSD tests on ANOVA results of normalized node degree and betweenness centrality per network.

2.11. Network stability analysis

We performed stability analysis on each network by iteratively removing up to 50 % of nodes by degree descending order (degree based attack) and calculating the natural connectivity as the mean eigenvalue derived from the graph spectrum at each step, as proposed by Peng and Wu (2016) with the formula $\bar{\lambda}(g) = \frac{ln\left(\frac{1}{N}\sum_{i=1}^{N} e^{\lambda i}\right)}{N - ln(N)}$, where $\bar{\lambda}(g)$ is the natural connectivity of the undirected graph g with N vertices and λ^i is the spectrum of g. The lower the absolute value of the slope, the lower the stability. This structural robustness measure allowed us to assess how rapidly natural connectivity decreased per site, reflecting the resistance of microbial community structure to extinction events. Throughout this paper the term 'stability' refers to this metric. Stability analysis was also performed on the random removal of nodes (random based attack) over 100 iterations and the mean slope was calculated per network (Fig. A5). Degree based attack is performed to assess the importance of highly connected nodes, a proxy of keystone taxa, on network structure. While removal of random nodes provides an indication on the overall robustness of alternative paths on network structure. To test the differences of stability, an ANCOVA followed by a pairwise comparisons between each pair of sites using the estimated marginal means with a bonferroni correction was performed (Supplementary file 5).

2.12. Topological roles of network nodes

We further evaluated the topological role of nodes in each network (bacterial, fungal and interdomain), particularly their structural role in the overall network, by classifying them according to their role in the network structure, as proposed by Olesen et al. (2007). Within module connectivity (Z_i) and among module connectivity (P_i) were calculated for each node i with the following equations: $Z_i = \frac{a_i - \overline{A}_s}{\sigma^s}$, where a_i is the number of intra-module connections of node i, $\overline{A}_s$ is the mean of intra-module connections in module s and σ^s is the standard deviation, $P_i = 1 - \sum_{s=1}^{N_m}\left(\frac{a_{is}}{a_i}\right)^2$, where a_{is} is the number of connections of node i in module s, even in it's own module, and a_i is the degree of node i. They were then classified as module hubs ($Z_i > 2.5$) which are structural to their own module, network hubs ($Z_i > 2.5$, $P_i > 0.62$) which are structural for their own module and overall network, connectors ($Z_i < 2.5$, $P_i > 0.62$) which connect different modules, and peripherals ($Z_i < 2.5$, $P_i < 0.62$) which has few links in their own and to other modules. Detailed properties of network and module hubs are provided in Supplementary files 6 and 7.

3. Results

3.1. Disturbance results in distinct soil cover and chemistry compared to natural environments

Firstly, the old farm (OF) and evaporation basin (EB), corresponding respectively to anthropic and natural disturbances, were mainly characterized by the presence of soil sealing or crusting resulting from the watering-drought succession pattern. This was confirmed by the XRF parameters as OF and EB clustered together and were explained by an increased proportion of K, Al, Ca, Mn and Fe (Fig. 1). These elements were characteristic of the topsoil induration layer, where intense flooding events followed by drought had enriched the surface with clay microparticles (Al, Fe and Mn enrichment). Secondly, Nat 1 and LR clustered together, and Nat 2 was separated from the other sites, with the chemical composition differences being explained by the increased proportion of Mg and Si. Natural environments (Nat 1, Nat 2) and restored land from anthropic disturbance (LR) were characterized by an increase in plant litter and surrounding vegetation (Fig. A6). Further details on the proportional enrichment of each element are available in the Supplementary information (Fig. A7).

3.2. Microbial diversity is highly impacted by natural long-term disturbance

The evaporation basin (EB), corresponding to a natural long-term disturbance, had the lowest bacterial and fungal alpha diversity. Differences in diversity between the natural sites (Nat1 and Nat 2) were greater than diversity differences between the former agricultural site (OF) and the restored site (LR) (Fig. 2.A and 2.B). For bacteria, EB had significantly lower ASV counts (Chao1) and Shannon diversity index in the rhizosphere than all other sites, except for Nat 2 (Fig. 2.A). EB also had significantly lower ASV counts and Shannon diversity than the natural environments (EB vs Nat 1: $p < 0.05$; EB vs Nat 2: $p < 0.01$) and restored land (EB vs LR: $p < 0.05$). Bacterial communities were more deterministic in their composition throughout our study as compared to

fungi, as indicated in Fig. 2.C and 2.D (Supplementary file 2: 16S residual PERMANOVA R2 = 0.539; ITS2 residual PERMANOVA R2 = 0.681). The site effect was a greater driver of community composition compared to the compartment effect (Supplementary file 2: 16S site PERMANOVA R2 = 0.211***; ITS site PERMANOVA R2 = 0132***; 16S compartment PERMANOVA R2 = 0.139***; ITS compartment PERMANOVA R2 = 0.089***).

3.3. Microbial network topological properties and stability across sites

Network analysis was used to assess how microbial interactions and stability changed across sites, revealing two distinct network structures: (1) Nat 1, Nat 2 and EB which had a similar structure; and conversely (2) LR and OF whose structures were also similar (Fig. 3.A and 3.B). The ratio of positive-to-negative edges was lower for past anthropic disturbances (Fig. 3.B: OF = 56,5 %, LR = 53.8 %), as compared to natural environments (Nat 1 = 63,3 %, Nat 2 = 69,1 %) and the evaporation basin (EB = 72,8 %). The modularity and average path length both declined for anthropic sites (OF and LR) as compared to natural ecosystems (Nat 1 and Nat 2), which were similar in this regard to the natural disturbance (EB). In soil rhizosphere bacterial networks, the node normalized degree was higher for both anthropic (OF, LR) and natural (EB) disturbances compared to natural ecosystems (Fig. 4.A). The normalized betweenness centrality was the lowest in anthropic disturbances (OF, LR) (Fig. 4.A).

As microbial communities interact with each other, cross domain networks allowed us to assess whether the addition of fungi to bacterial networks resulted in topological changes, thus reflecting changes in microbial interactions. The addition of fungi to the networks resulted in similar patterns between sites for betweenness centrality (Fig. 4.A) as compared to bacterial networks. However, addition of fungi resulted in OF having the same normalized degree as natural environments.

We performed a stability analysis based on natural connectivity to test the network resistance. This allowed us to artificially observe how the network structure was impacted when nodes were removed, and thus determine if paths were redundant enough to be resistant to extinction (see Methods). Stability analysis revealed that in bacterial rhizosphere networks (Fig. 4.B), both Nat 1 and Nat 2 had the greatest stability (slope = −0.00209 and − 0.002, respectively), whereas OF had the lowest stability (slope = −0.00698), followed by LR (slope = −0.00462) and EB (slope = −0.00392). An interesting pattern we noted here concerned the intermediate stability of EB and LR networks, which both contrasted with the sharp decrease of natural connectivity for OF. Moreover, the addition of fungi in cross domain networks (Fig. 4.B) resulted in EB having the highest stability (slope = −0.00254), followed by natural environments (Nat 1 = −0.00418; Nat 2 = −0.00315), while OF and LR had the lowest stability (slope = −0.00687, slope = −0.00869, respectively). Random based attacks are presented in SI (Fig. A5), where only anthropic disturbances (OF, LR) for both bacteria and cross domain networks, had a low network stability. This indicates that their network structure is vulnerable to failure, where redundancy of path is not sufficient enough to maintain network structure following random extinction. Disturbances also impacted the inter- and intra-kingdom positive and negative edge ratios (Fig. 4.C). Natural environments (Nat 1, Nat 2) had a higher proportion of positive fungal links (12.7 % and 13.5 %, respectively) than disturbed environments (OF: 2.3 %, EB: 4.7 %, LR: 4.8 %). The same pattern was noted for negative fungal links, i.e., proportionally twofold more abundant in natural ecosystems (Nat 1: 4.4 %, Nat 2: 5.1 %, OF: 1.0 %, EB: 2.1 %, LR: 2.3 %). Finally, positive bacterial links were more prevalent in EB (47.9 %) and OF (42.4 %) than in LR (33.9 %) and natural ecosystems (Nat 1: 34.2 %, Nat 2: 29.8 %).

3.4. Topological properties of nodes and keystones ASVs

To identify potential keystone ASVs defined here as ASVs which, regardless of their relative abundance, had a fundamental network structure role (i.e., network or module hubs), and thus potentially in the ecosystem, nodes were classified according to their topological properties (i.e., within-module connectivity Z_i and among-module connectivity P_i). This classification revealed a strong pattern across sites, as overall network topology. For bacterial rhizosphere networks (Fig. 5.A), natural

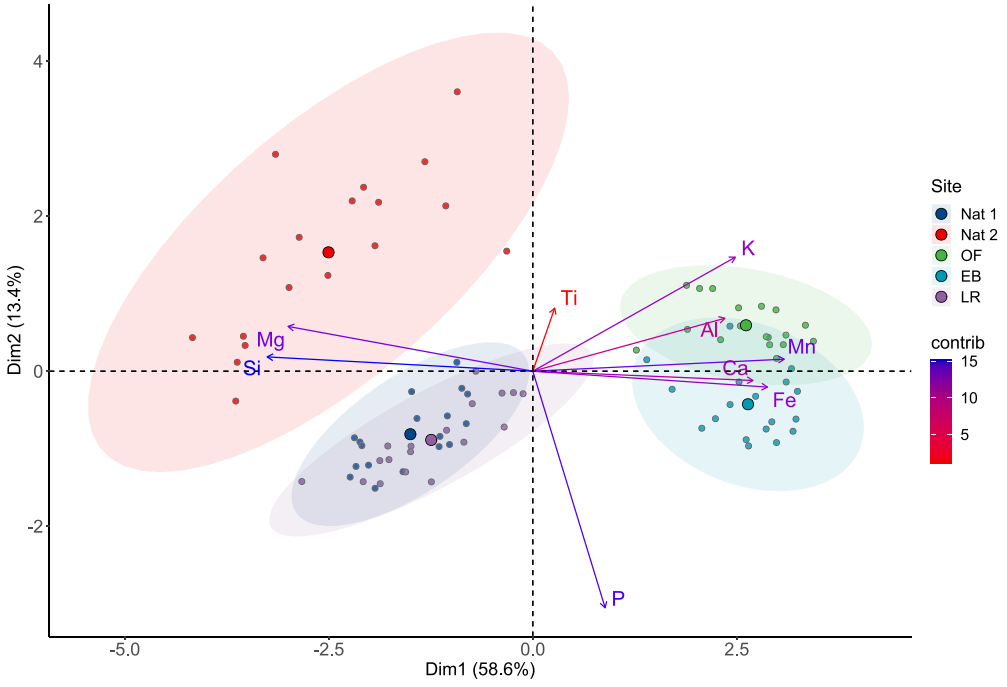

Fig. 1. Disturbance impact soil chemistry. Principal component analysis (PCA) of clr-transformed XRF soil parameters. Colors represent sites (Nat 1, Nat 2 = natural ecosystems; OF = old Farm; EB = evaporation basin; LR = land reclamation), and vectors are colored according to their contributions. Dimension 1 explains 58.6 % of the variance, while dimension 2 explains 13.4 %.

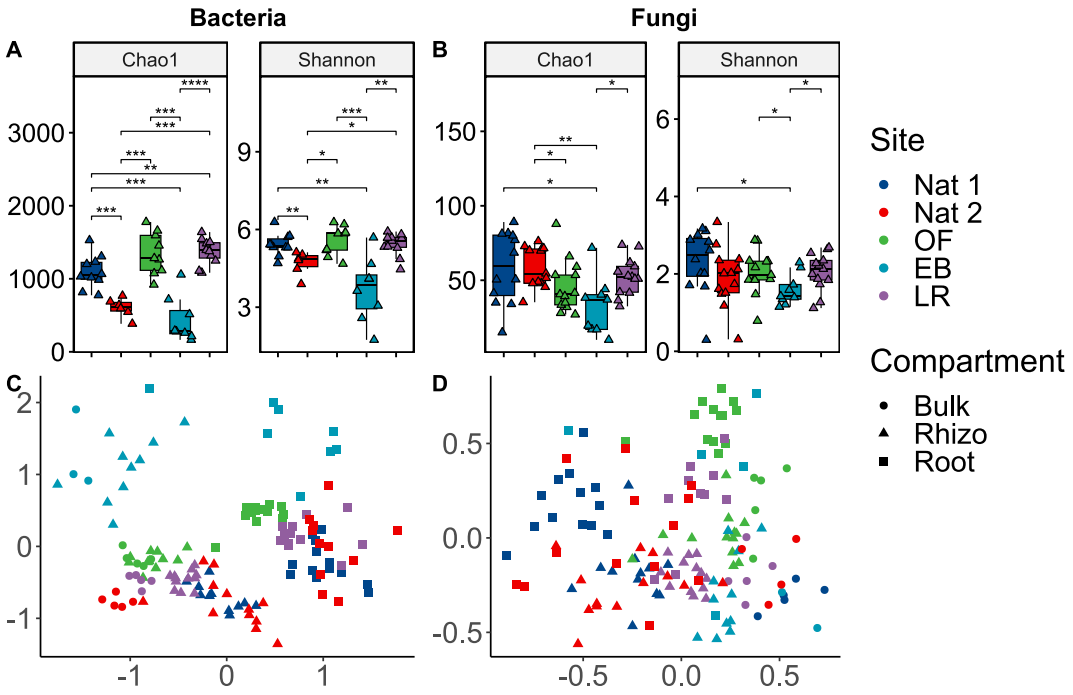

Fig. 2. Microbial community composition and diversity is impacted by disturbances. Chao and Shannon diversity indexes for bacteria (A) and fungi (B) in the rhizosphere across sites (Nat 1, Nat 2 = natural ecosystems; OF = old farm; EB = evaporation basin; LR = land reclamation). Analyses were performed on rarefied ASV matrices at 5000 reads for samples with at least 5000 reads. Significance levels of the Wilcoxon tests are represented between each site by stars for significantly different paired groups (* = $p < 0.05$; ** = $p < 0.01$; *** = $p < 0.001$; **** = $p < 0.0001$). Non-metric multidimensional scaling (NMDS) of samples according to compartment and sites for bacteria (C) and fungi (D) across sites and compartments. Samples with <3000 reads were discarded. Analyses were performed on Bray-Curtis distances on Hellinger transformed matrices. Stress values are 0.16 for 16S (k = 2) and 0.19 for ITS (k = 3).

environments (Nat 1, Nat 2) and EB exhibited one module hub with a relatively steady proportion of connectors and peripheral nodes. Otherwise, OF and LR exhibited several network hubs and a higher proportion of connectors (Supplementary file 7). As for the node degree and betweenness centrality distribution, the addition of fungi generated results similar to those of bacteria only networks, with the exception of Nat 2 which had no module hubs or network hubs (Fig. 5.B). Actinobacteriota were the most common bacterial network hubs (taxonomical information and network properties of node are detailed in Supplementary file 6). Another interesting feature concerned the systematic low relative abundance of all ASVs classified as networks or module hubs (Fig. A8).

4. Discussion

Soil microbial communities play key roles in ecosystem functioning (Wagg et al., 2019) while markedly responding to disturbances (Hernandez et al., 2021). However, the impact on microbial co-occurrence patterns in response to different land uses and the effects of anthropic versus natural disturbances on microbiome resilience have yet to be studied in detail. In the present study, both disturbances were found to be linked to specific hydric regimes, characterized by wetting-desiccation successions occurring infrequently over a long-time span in the evaporation basin, while more frequently over a shorter time span on a former agricultural site. Indeed, a previous disturbance can induce a legacy effect on the soil microorganism composition (Meisner et al., 2018), which may increase microbiome resistance to subsequent disturbance. For example, Evans and Wallenstein (2014) showed that an increased frequency of drying-rewetting stress in an experimental field resulted in a greater proportion of tolerant bacterial taxa, suggesting bacterial life strategy adaptation to stress over time. The findings of our study, which was carried out in a natural arid environment, suggested that these disturbances were due to a temporally driven hydric constraint (wetting-desiccation succession), as water is known to be a direct (e.g. seasonal rainfall, aridity) and indirect (e.g. salinity, plant cover, pH) driver of arid soil microbiome composition and functionality (Maestre et al., 2015; Shen et al., 2021). In this study, we showed that the response of bacteria and fungi differed in magnitude across the five sites and that that the microbial network, topology, structure and stability driven by a naturally occurring disturbance was closer to that found in a natural environment than in one impacted by anthropic disturbance. This suggests that the temporal context of a disturbance is a key driver of microbial co-occurrence stability, with short-term disturbances inducing less stability than long-term disturbances. However, as our study includes few or no site replication, and as natural environments are variable and subject to different constraints, it is important to remember that these results will need to be consolidated by other studies.

4.1. Lower microbial diversity only in the natural disturbance conditions

The alpha and beta diversity responses were not consistently significant throughout the land uses. This was also noted by Xu et al. (2022) and Yu et al. (2022) who found no impact of land use type on bacterial and fungal alpha diversity. Moreover, Banerjee et al. (2019) showed that agricultural intensification under both organic and conventional farming conditions had no effect on alpha diversity, but the structure of the networks, especially their connectivity, was higher under organic farming—a topology characteristic of higher resistance (Santolini and Barabási, 2018). These results contrast with those of other studies that showed a significant effect of land use types on soil microbial diversity (Jiao et al., 2021; Karimi et al., 2019; Turley et al., 2020). Overall, these contrasted results shed light on microbial diversity as an insufficient proxy of microbiome response to disturbance.

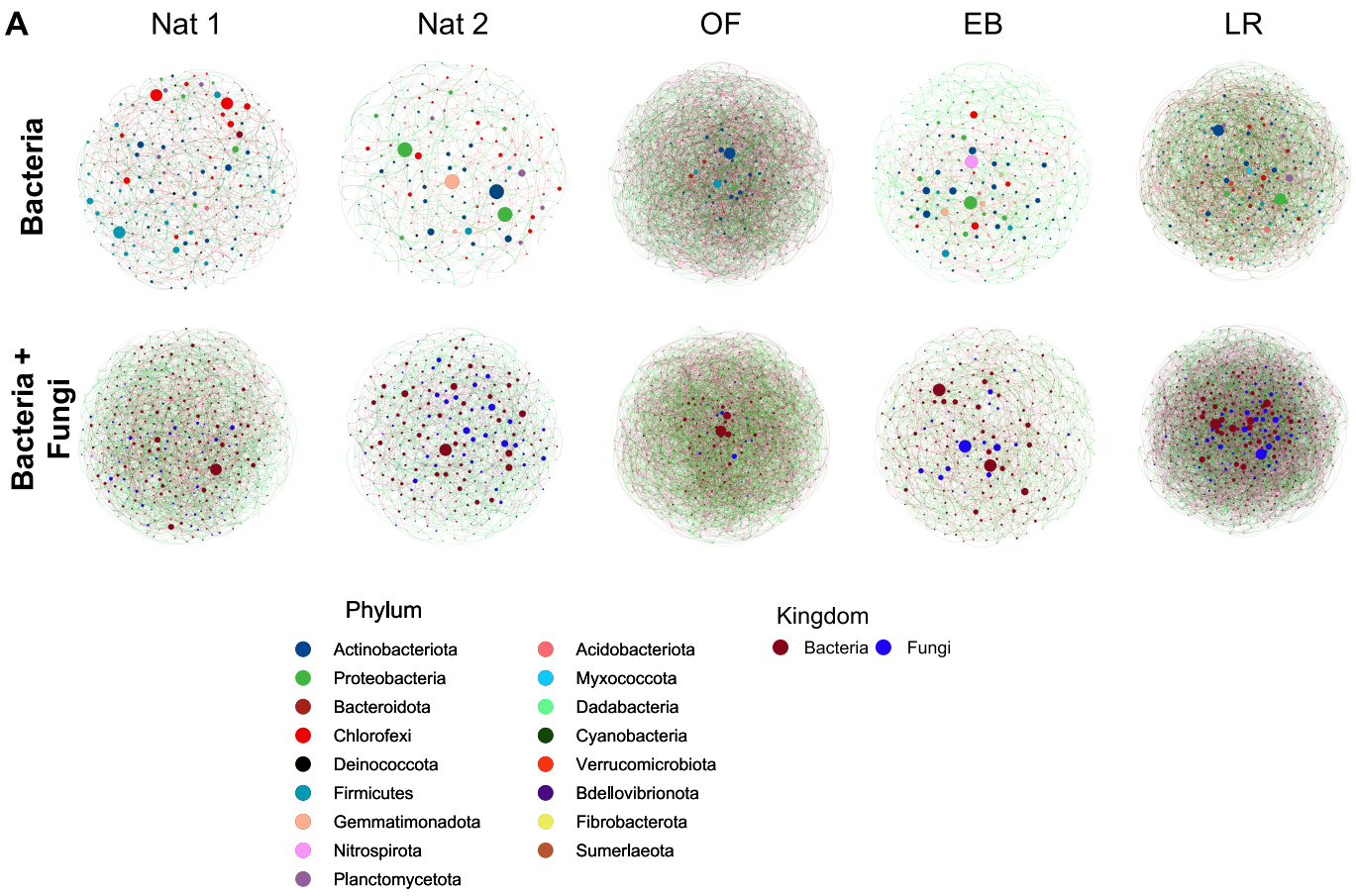

B

	Network type	Vertex	Edge	Average degree	Average path length	Modularity	Positive edges (%)	Negative edges (%)
Nat 1	Bacteria	309	892	5.77	3.78	0.67	63.44	36.66
Nat 2	Bacteria	212	450	4.25	4.19	0.73	69.11	30.89
OF	Bacteria	573	3718	12.98	2.91	0.44	56.48	43.52
EB	Bacteria	294	935	6.36	3.67	0.64	72.83	27.17
LR	Bacteria	509	2778	10.92	2.99	0.48	53.85	46.15

	Network type	Vertex	Edge	Average degree	Average path length	Modularity	Positive edges (%)	Negative edges (%)
Nat 1	Bacteria + Fungi	464	2276	9.81	3.11	0.53	62.30	37.70
Nat 2	Bacteria + Fungi	337	1194	7.09	3.37	0.59	66.83	33.17
OF	Bacteria + Fungi	665	4618	13.89	2.96	0.48	56.17	43.83
EB	Bacteria + Fungi	345	1364	7.91	3.50	0.60	68.48	31.52
LR	Bacteria + Fungi	664	4746	14.74	2.79	0.41	54.83	45.17

Fig. 3. Network topology between natural environments and natural disturbance is distinct from anthropic disturbance. (A) Bacterial rhizosphere SPIEC-EASI networks across sites. Different node colors represent different phyla and the node size is exponentially proportional to the degree (exponential spline in Gephi). Green edges represent positive covariance between nodes, while red edges represent negative covariance. Networks were constructed using ASVs with a sum >50 and prevalence >20 %. Samples with <5000 reads were discarded. SPIEC-EASI was run with neighborhood selection (MB) with 999 cross-validation permutations, and the stability approach to regularization selection (StARS) was used to construct the most stable network along a lambda path of 99 iterations per permutation, with a lambda min ratio of 0.01 (A). Cross domain SPIEC-EASI co-variance networks across sites. Different node colors represent different kingdoms. The network construction parameters were the same as single domain networks. (B) Topological features of the co-occurrence networks (bacteria only and bacteria + fungi).

4.2. Microbial network structure and stability is context dependent when impacted by disturbance

Stable networks are characterized by high modularity, where species interact more within their module than with other groups (Olesen et al., 2007). This enables communities to withstand disturbances by limiting extinction or decrease in ASV abundance to spread to different modules, as they share fewer links with the former (Baldassano and Bassett, 2016; Stouffer and Bascompte, 2011). In our study, network modularity was correlated with the stability analysis findings (in both bacteria and bacteria-fungi networks: Spearman's $\rho = 1$, $p = 0.01667$). Hence, past short-term anthropic disturbances, is characterized by low modularity

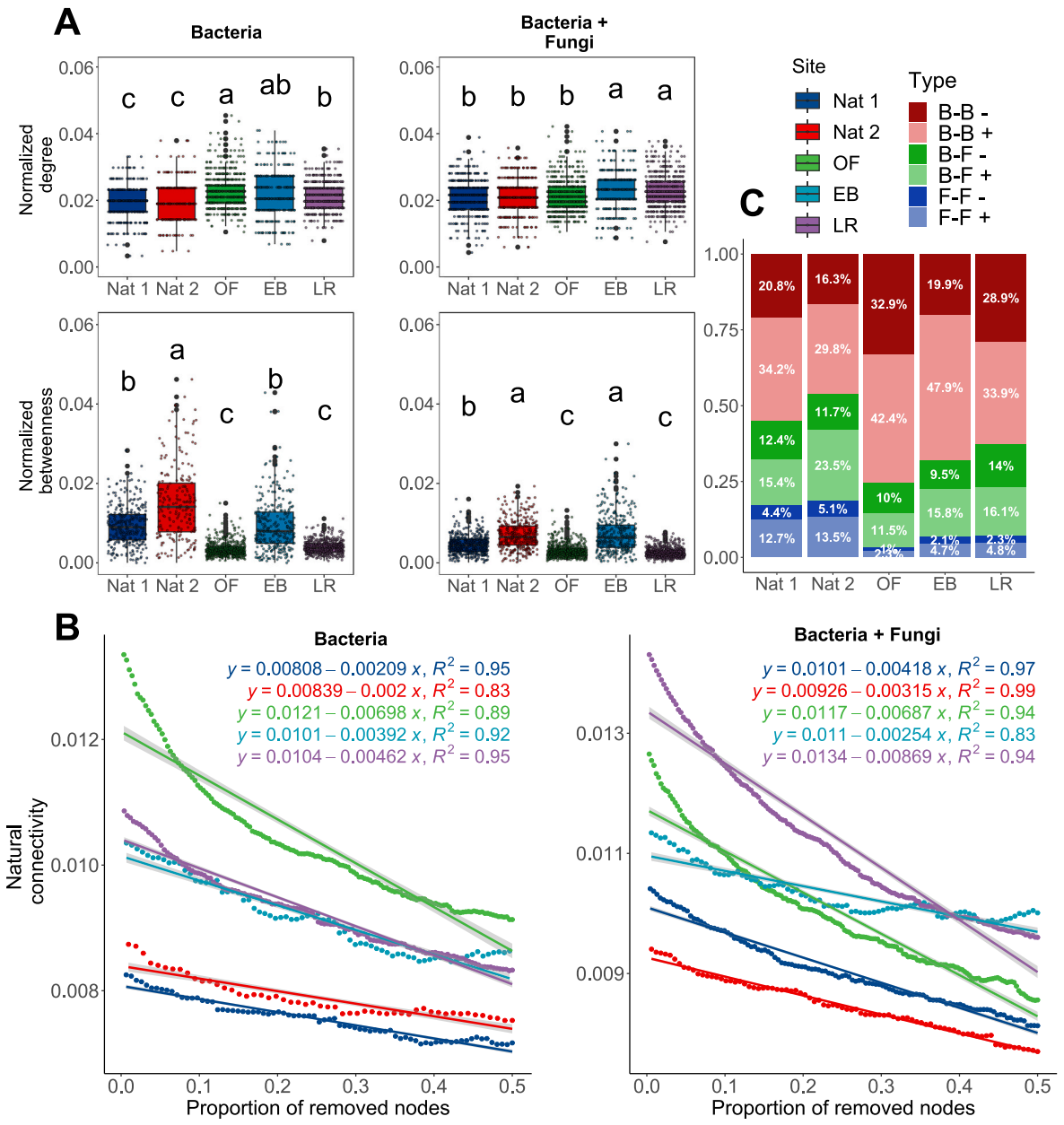

Fig. 4. Bacterial network stability is higher in natural environments than both natural and anthropic disturbances and fungi stabilize cross-domain networks in the natural disturbance. (A) Boxplots of normalized node degree and normalized betweenness centrality per site for bacterial rhizospheric soil networks and cross domain networks (bacteria + fungi). Different letters represent significant differences between sites according to the Tukey honest significant differences test performed on ANOVA results. (B) Changes in network stability based on natural connectivity changes along iterative removal of nodes, up to 50 %, in each network. The slope is indicated with associated R2. The higher the slope value, the greater the stability. (C) Edge number and proportion for each bacteria + fungi networks according to site. Edges are separated by positive or negative covariance values (+, −) and by inter- and intra-kingdom links (B = bacteria, F = fungi).

and the lowest stability in comparison to natural environments and long-term natural disturbance. Natural environments and disturbance also exhibited a higher average path length, correlated with the higher stability (again, in both bacteria and bacteria + fungi networks: Spearman's $\rho = 1$, $p = 0.01667$). One underlying mechanism could involve mitigation of the disturbance to spread from one node to others in the network, induced by positive feedbacks loops (Coyte et al., 2015). Whether these modular structures represent biotic interactions among ASVs or niche partitioning has yet to be confirmed. Yet this may indicate that local microbial communities coping with long-term stress in the evaporation basin were able to gradually adapt to edaphic and hydric constraints, while past agronomic activities prompted drastic reorganization of microbial communities. Although beyond the scope of this study, adaptation and interactions are known to be interrelated in complex biological communities where biotic interactions could modify species' evolutionary responses (Barraclough, 2015; Turcotte et al., 2012). Lower stability in disturbed sites may reflect the fact that some maladapted microbial communities were undergoing evolutionary adaptation to new niche requirements, known to be instable in the first step (Hillesland and Stahl, 2010). Shedding light on evolutionary responses and mechanisms of microbiomes coping with disturbances in an interaction framework could generate valuable information on microbial stress assembly in the future.

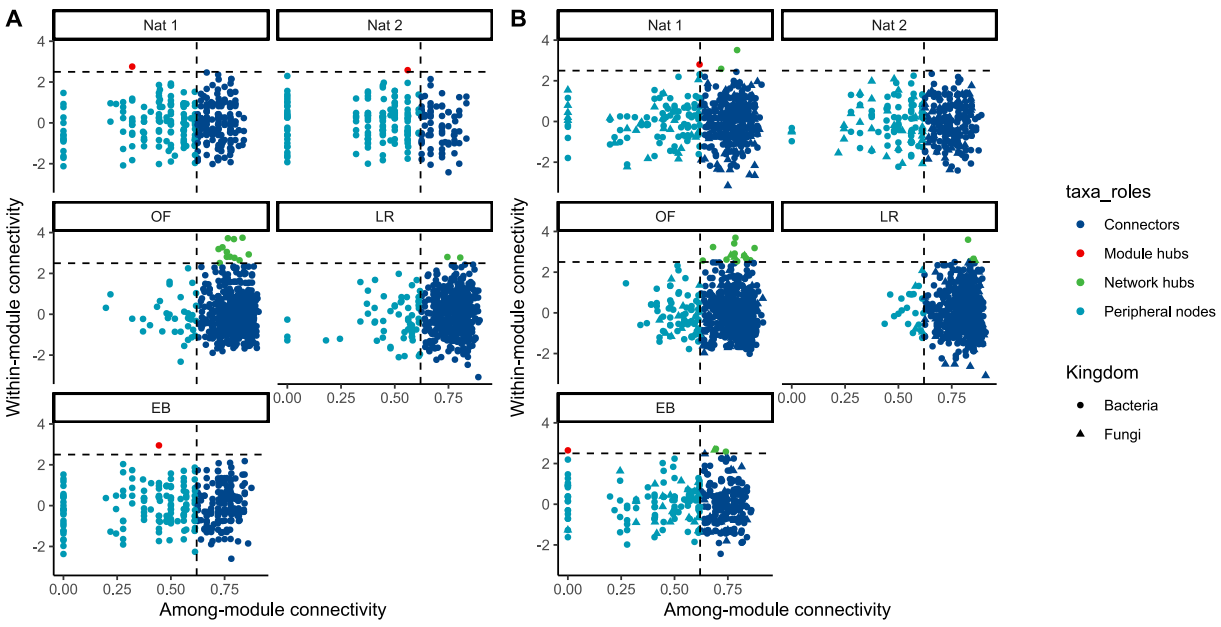

Fig. 5. Network nodes topology in networks is consistent with the disturbance across bacteria and bacteria + fungi interaction. Classification of nodes to identify taxa roles in network structures for bacteria (A) and bacteria + fungi (B) soil rhizosphere networks per site. Bacteria are represented by round dots and fungi by triangular dots. Nodes or ASV are plotted according to among-module connectivity (P) against within-module connectivity (Z). Module hubs have Z > 2.50, connectors have $P > 0.62$, Network hubs have both Z > 2.50 and P > 0.62, peripheral nodes have both Z < 2.50 and $P < 0.62$.

4.3. Fungi mediate bacterial interactions and network stability

In the evaporation basin, cross domain networks displayed higher stability compared to bacterial networks. This reflects the high resistance of fungi in microbial networks impacted by hydric constraints, particularly with regard to wetting-desiccation successions. The resistance of fungal communities to desiccation has been reported by Barnard et al. (2013), who showed that fungi had a high degree of resistance to desiccation-rewetting in a simulated rainfall experiment in a Mediterranean grassland in California. In some cases, fungi can even improve bacterial resistance to hydric stress, as shown by Hestrin et al. (2022), where *R. irregularis* and *S. bescii* endomycorrhizal fungi inoculation had a protective effect on several hyphosphere bacterial phyla under water limiting conditions. We also found a signature preferential inter-kingdom relationship between fungi and bacteria at all of our sites, where fungi predominantly coexisted though inter- rather than intra-kingdom relationships. Yu et al. (2022) hypothesized that this phenomenon reflected environmental-related filtration process, while noting a similar pattern in a floodplain ecosystem. This highlights the importance of fungi in microbial food webs, and their relation with other microbial kingdoms, particularly in nutrient and water depleted desert ecosystems.

4.4. Bacterial interactions support the stress-gradient hypothesis

The stress-gradient hypothesis (Bertness and Callaway, 1994) is an ecological framework which stipulates that increased stress leads to increased positive interactions. Our results were in line with this hypothesis with regard to bacterial interactions as the disturbed ecosystems had more positive bacteria-to-bacteria interactions. This was not the case for positive fungi-to-fungi or bacteria-to-fungi interactions, as confirmed by the high response of the bacterial microbiome to disturbances, contrary to the fungal microbiome (Barnard et al., 2013; Gao et al., 2022; Sun et al., 2017). An increase in negative microbial interactions in former agricultural sites could be explained by environmental filtering, where land use changes on old farms could result in divergent niche requirements following the abandonment of irrigation and agricultural practices. This transitional state of microbial populations following the abandonment of agricultural practices could prompt microbial populations to shift from being copiotrophs to being oligotrophs, as is often the case in secondary successions following disturbances (Barnard et al., 2013; Sun et al., 2017).

5. Conclusion and perspectives

Our study provides the first evidence that natural disturbance, occurring over a long-time span, exhibited a similar microbial network structure and stability as in natural environments, suggesting an adaptation of microbial interactions upon exposure to repeated long-term stress. Conversely, the anthropic disturbance characterized in our study by past agricultural activity had detrimental effects on network stability, even after natural recovery. We also highlighted the mitigating effect of fungal communities regarding the stability of inter-kingdom networks in a naturally occurring disturbance setting, thereby highlighting the relevance of fungal-bacterial interactions in soil microbiome stress alleviation. The relative evolutionary rate has been found to be habitat-dependent, with microbial communities evolving faster in extreme environments (Li et al., 2014), but future research is needed to assess the evolutionary trajectories of microbial communities coping with abiotic stress in a complex natural environment, and to determine the extent to which interactions modulate this evolutionary adaptation and temporality.

Funding

This work was supported supported by the SoFunLand project, part of the Oasis program funded under the partnership between the RCU (Royal Commission for AlUla) and AFALULA (Agence Française pour le development d'AlUla).

CRediT authorship contribution statement

Kenji Maurice: Conceptualization, Methodology, Investigation, Data curation, Writing – original draft, Writing – review & editing, Visualization. **Amélia Bourceret:** Software, Data curation, Writing – review & editing. **Sami Youssef:** Resources. **Stéphane Boivin:** Writing

– review & editing. **Liam Laurent-Webb:** Writing – review & editing. **Coraline Damasio:** Investigation. **Hassan Boukcim:** Supervision, Project administration, Funding acquisition, Writing – review & editing. **Marc-André Selosse:** Supervision, Project administration, Funding acquisition. **Marc Ducousso:** Conceptualization, Supervision, Project administration, Funding acquisition, Writing – review & editing.

Declaration of competing interest

The authors declare that they have no known competing financial interests or personal relationships that could have appeared to influence the work reported in this paper.

Supplementary data to this article can be found online at https://doi.org/10.1016/j.scitotenv.2023.167969.

Data availability

Demultiplexed sequence data are available at NCBI (Bio-project PRJNA1028866, Biosamples SAMN37854590 to SAMN37854744). Soil XRF raw datas are available in Supplementary file 1. Extended PERMANOVA are available in Supplementary file 2. Phylum level of positive and negative interactions proportion for each bacteria network are listed in Supplementary file 3. Phylum level of positive and negative interactions proportion for each bacteria-fungi networks are listed in Supplementary file 4. ANCOVA results for the stability analysis of each network with the paired comparisons with the estimated marginal means method is available in Supplementary file 5. Module and network hubs taxonomical information, topology, Z_i and P_i values are listed in Supplementary file 6. Proportion of taxa roles in each network is available in Supplementary file 7.

Acknowledgement

We would like to thank all those involved in the SoFunLand project, and the RCU (Royal Commission for AlUla) and Afalula (Agence Française pour le Developpement d'AlUla) for their financial support. We would also like to thank O. Domergue, R. Destabel and A. Dehail for their help with soil and biomolecular analyses. And our invaluable local guide Abdulaziz Marzouq Salman AlNajem for his knowledge of the field. Finally, we would like to thank A. Camuel for her advice on the manuscript and D. Manley for his English proofing.

References

Aitchison, J., 1981. A new approach to null correlations of proportions. Math. Geol. 13, 175–189. https://doi.org/10.1007/BF01031393.

Baldassano, S.N., Bassett, D.S., 2016. Topological distortion and reorganized modular structure of gut microbial co-occurrence networks in inflammatory bowel disease. Sci. Rep. 6, 26087. https://doi.org/10.1038/srep26087.

Banerjee, S., Walder, F., Büchi, L., Meyer, M., Held, A.Y., Gattinger, A., Keller, T., Charles, R., van der Heijden, M.G.A., 2019. Agricultural intensification reduces microbial network complexity and the abundance of keystone taxa in roots. ISME J. 13, 1722–1736. https://doi.org/10.1038/s41396-019-0383-2.

Barberán, A., Bates, S.T., Casamayor, E.O., Fierer, N., 2012. Using network analysis to explore co-occurrence patterns in soil microbial communities. ISME J. 6, 343–351. https://doi.org/10.1038/ismej.2011.119.

Bardgett, R.D., van der Putten, W.H., 2014. Belowground biodiversity and ecosystem functioning. Nature 515, 505–511. https://doi.org/10.1038/nature13855.

Barnard, R.L., Osborne, C.A., Firestone, M.K., 2013. Responses of soil bacterial and fungal communities to extreme desiccation and rewetting. ISME J. 7, 2229–2241. https://doi.org/10.1038/ismej.2013.104.

Barraclough, T.G., 2015. How do species interactions affect evolutionary dynamics across whole communities? Annu. Rev. Ecol. Evol. Syst. 46, 25–48. https://doi.org/10.1146/annurev-ecolsys-112414-054030.

Berendsen, R.L., Pieterse, C.M.J., Bakker, P.A.H.M., 2012. The rhizosphere microbiome and plant health. Trends Plant Sci. 17, 478–486. https://doi.org/10.1016/j.tplants.2012.04.001.

Berry, D., Widder, S., 2014. Deciphering microbial interactions and detecting keystone species with co-occurrence networks. Front. Microbiol. 5 https://doi.org/10.3389/fmicb.2014.00219.

Bertness, M.D., Callaway, R., 1994. Positive interactions in communities. Trends Ecol. Evol. 9, 191–193. https://doi.org/10.1016/0169-5347(94)90088-4.

Blondel, V.D., Guillaume, J.L., Lambiotte, R., Lefebvre, E., 2008. Fast unfolding of communities in large networks. J. Stat. Mech. Theory Exp. 2008 (10), 10008.

Cameron, E.S., Schmidt, P.J., Tremblay, B.J.-M., Emelko, M.B., Müller, K.M., 2021. Enhancing diversity analysis by repeatedly rarefying next generation sequencing data describing microbial communities. Sci. Rep. 11, 22302. https://doi.org/10.1038/s41598-021-01636-1.

Cavicchioli, R., Ripple, W.J., Timmis, K.N., Azam, F., Bakken, L.R., Baylis, M., Behrenfeld, M.J., Boetius, A., Boyd, P.W., Classen, A.T., Crowther, T.W., Danovaro, R., Foreman, C.M., Huisman, J., Hutchins, D.A., Jansson, J.K., Karl, D.M., Koskella, B., Mark Welch, D.B., Martiny, J.B.H., Moran, M.A., Orphan, V.J., Reay, D. S., Remais, J.V., Rich, V.I., Singh, B.K., Stein, L.Y., Stewart, F.J., Sullivan, M.B., van Oppen, M.J.H., Weaver, S.C., Webb, E.A., Webster, N.S., 2019. Scientists' warning to humanity: microorganisms and climate change. Nat. Rev. Microbiol. 17, 569–586. https://doi.org/10.1038/s41579-019-0222-5.

Coyte, K.Z., Schluter, J., Foster, K.R., 2015. The ecology of the microbiome: networks, competition, and stability. Science 350, 663–666. https://doi.org/10.1126/science.aad2602.

Csardi, G., Nepusz, T., 2006. The igraph software package for complex network research. Inter. J. Compl. Syst. 1695 (5), 1–9.

Davis, N.M., Proctor, D.M., Holmes, S.P., Relman, D.A., Callahan, B.J., 2018. Simple statistical identification and removal of contaminant sequences in marker-gene and metagenomics data. Microbiome 6, 226. https://doi.org/10.1186/s40168-018-0605-2.

de Vries, F.T., Liiri, M.E., Bjørnlund, L., Bowker, M.A., Christensen, S., Setälä, H.M., Bardgett, R.D., 2012. Land use alters the resistance and resilience of soil food webs to drought. Nat. Clim. Chang. 2, 276–280. https://doi.org/10.1038/nclimate1368.

de Vries, F.T., Grif, R.I., Gweon, H.S., Hallin, S., Kaisermann, A., Keith, A.M., Kretzschmar, M., Lemanceau, P., Lumini, E., Mason, K.E., Oliver, A., Ostle, N., Prosser, J.I., Thion, C., Thomson, B., Bardgett, R.D., 2018. Soil bacterial networks are less stable under drought than fungal networks. Nat. Commun. 12.

Delgado-Baquerizo, M., Doulcier, G., Eldridge, D.J., Stouffer, D.B., Maestre, F.T., Wang, J., Powell, J.R., Jeffries, T.C., Singh, B.K., 2020. Increases in aridity lead to drastic shifts in the assembly of dryland complex microbial networks. Land Degrad. Dev. 31, 346–355. https://doi.org/10.1002/ldr.3453.

Evans, S.E., Wallenstein, M.D., 2014. Climate change alters ecological strategies of soil bacteria. Ecol. Lett. 17, 155–164. https://doi.org/10.1111/ele.12206.

Gao, C., Xu, L., Montoya, L., Madera, M., Hollingsworth, J., Chen, L., Purdom, E., Singan, V., Vogel, J., Hutmacher, R.B., Dahlberg, J.A., Coleman-Derr, D., Lemaux, P. G., Taylor, J.W., 2022. Co-occurrence networks reveal more complexity than community composition in resistance and resilience of microbial communities. Nat. Commun. 13, 3867. https://doi.org/10.1038/s41467-022-31343-y.

Goberna, M., Verdú, M., 2022. Cautionary notes on the use of co-occurrence networks in soil ecology. Soil Biol. Biochem. 166, 108534 https://doi.org/10.1016/j.soilbio.2021.108534.

Hassani, M.A., Durán, P., Hacquard, S., 2018. Microbial interactions within the plant holobiont. Microbiome 6, 58. https://doi.org/10.1186/s40168-018-0445-0.

Hernandez, D.J., David, A.S., Menges, E.S., Searcy, C.A., Afkhami, M.E., 2021. Environmental stress destabilizes microbial networks. ISME J. 15, 1722–1734. https://doi.org/10.1038/s41396-020-00882-x.

Hestrin, R., Kan, M., Lafler, M., Wollard, J., Kimbrel, J.A., Ray, P., Blazewicz, S.J., Stuart, R., Craven, K., Firestone, M., Nuccio, E.E., Pett-Ridge, J., 2022. Plant-associated fungi support bacterial resilience following water limitation. ISME J. 16, 2752–2762. https://doi.org/10.1038/s41396-022-01308-6.

Hillesland, K.L., Stahl, D.A., 2010. Rapid evolution of stability and productivity at the origin of a microbial mutualism. Proc. Natl. Acad. Sci. U. S. A. 107, 2124–2129. https://doi.org/10.1073/pnas.0908456107.

Hirano, H., Takemoto, K., 2019. Difficulty in inferring microbial community structure based on co-occurrence network approaches. BMC Bioinform. 20, 329. https://doi.org/10.1186/s12859-019-2915-1.

Högfors-Rönnholm, E., Christel, S., Engblom, S., Dopson, M., 2018. Indirect DNA extraction method suitable for acidic soil with high clay content. MethodsX 5, 136–140. https://doi.org/10.1016/j.mex.2018.02.005Hubbard.

Hubbard, C.J., Li, B., McMinn, R., Brock, M.T., Maignien, L., Ewers, B.E., Kliebenstein, D., Weinig, C., 2019. The effect of rhizosphere microbes outweighs host plant genetics in reducing insect herbivory. Mol. Ecol. 28, 1801–1811. https://doi.org/10.1111/mec.14989.

Jansson, J.K., Hofmockel, K.S., 2020. Soil microbiomes and climate change. Nat. Rev. Microbiol. 18, 35–46. https://doi.org/10.1038/s41579-019-0265-7.

Jiao, S., Zhang, B., Zhang, G., Chen, W., Wei, G., 2021. Stochastic community assembly decreases soil fungal richness in arid ecosystems. Mol. Ecol. 30, 4338–4348. https://doi.org/10.1111/mec.16047.

Karimi, B., Maron, P.A., Chemidlin-Prevost Boure, N., Bernard, N., Gilbert, D., Ranjard, L., 2017. Microbial diversity and ecological networks as indicators of environmental quality. Environ. Chem. Lett. 15, 265–281. https://doi.org/10.1007/s10311-017-0614-6.

Karimi, B., Dequiedt, S., Terrat, S., Jolivet, C., Arrouays, D., Wincker, P., Cruaud, C., Bispo, A., Chemidlin Prévost-Bouré, N., Ranjard, L., 2019. Biogeography of soil bacterial networks along a gradient of cropping intensity. Sci. Rep. 9, 3812. https://doi.org/10.1038/s41598-019-40422-y.

Kõljalg, U., Nilsson, H.R., Schigel, D., Tedersoo, L., Larsson, K.-H., May, T.W., Taylor, A. F.S., Jeppesen, T.S., Frøslev, T.G., Lindahl, B.D., Põldmaa, K., Saar, I., Suija, A., Savchenko, A., Yatsiuk, I., Adojaan, K., Ivanov, F., Piirmann, T., Pöhönen, R., Zirk, A., Abarenkov, K., 2020. The taxon hypothesis paradigm—on the unambiguous detection and communication of taxa. Microorganisms 8, 1910. https://doi.org/10.3390/microorganisms8121910.

Kurtz, Z.D., Müller, C.L., Miraldi, E.R., Littman, D.R., Blaser, M.J., Bonneau, R.A., 2015. Sparse and compositionally robust inference of microbial ecological networks. PLoS Comput. Biol. 11, e1004226 https://doi.org/10.1371/journal.pcbi.1004226.

Kuypers, M.M.M., Marchant, H.K., Kartal, B., 2018. The microbial nitrogen-cycling network. Nat. Rev. Microbiol. 16, 263–276. https://doi.org/10.1038/nrmicro.2018.9.

Li, S.-J., Hua, Z.-S., Huang, L.-N., Li, J., Shi, S.-H., Chen, L.-X., Kuang, J.-L., Liu, J., Hu, M., Shu, W.-S., 2014. Microbial communities evolve faster in extreme environments. Sci. Rep. 4, 6205. https://doi.org/10.1038/srep06205.

Liu, L.-N., Razaq, A., Atri, N.S., Bau, T., Belbahri, L., Bouket, A.C., Chen, L.-P., Deng, C., Ilyas, S., Khalid, A.N., Kitaura, M.J., Kobayashi, T., Li, Y., Lorenz, A.P., Ma, Y.-H., Malysheva, E., Malysheva, V., Nuytinck, J., Qiao, M., Saini, M.K., Scur, M.C., Sharma, S., Shu, L.-L., Spirin, V., Tanaka, Y., Tojo, M., Uzuhashi, S., Valerio-Junior, C., Verbeken, A., Verma, B., Wu, R.-H., Xu, J.-P., Yu, Z.-F., Zeng, H., Zhang, B., Banerjee, A., Beddiar, A., Bordallo, J.-J., Dafri, A., Dima, B., Krisai-Greilhuber, I., Lorenzini, M., Mandal, R., Morte, A., Nath, P.S., Papp, V., Pavlik, J., Rodriguez, A., Sevcikova, H., Urban, A., Voglmayr, H., Zapparoli, G., 2018. Fungal systematics and evolution: FUSE 4. SYDOWIA. https://doi.org/10.12905/0380.sydowia70-2018-0211.

Maestre, F.T., Delgado-Baquerizo, M., Jeffries, T.C., Eldridge, D.J., Ochoa, V., Gozalo, B., Quero, J.L., García-Gómez, M., Gallardo, A., Ulrich, W., Bowker, M.A., Arredondo, T., Barraza-Zepeda, C., Bran, D., Florentino, A., Gaitán, J., Gutiérrez, J. R., Huber-Sannwald, E., Jankju, M., Mau, R.L., Miriti, M., Naseri, K., Ospina, A., Stavi, I., Wang, D., Woods, N.N., Yuan, X., Zaady, E., Singh, B.K., 2015. Increasing aridity reduces soil microbial diversity and abundance in global drylands. Proc. Natl. Acad. Sci. U. S. A. 112, 15684–15689. https://doi.org/10.1073/pnas.1516684112.

Malik, A.A., Puissant, J., Buckeridge, K.M., Goodall, T., Jehmlich, N., Chowdhury, S., Gweon, H.S., Peyton, J.M., Mason, K.E., van Agtmaal, M., Blaud, A., Clark, I.M., Whitaker, J., Pywell, R.F., Ostle, N., Gleixner, G., Griffiths, R.I., 2018. Land use driven change in soil pH affects microbial carbon cycling processes. Nat. Commun. 9, 3591. https://doi.org/10.1038/s41467-018-05980-1.

Martin, M., 2011. Cutadapt removes adapter sequences from high-throughput sequencing reads. EMBnet J. 17, 10. https://doi.org/10.14806/ej.17.1.200.

McMurdie, P.J., Holmes, S., 2014. Waste not, want not: why rarefying microbiome data is inadmissible. PLoS Comput. Biol. 10, e1003531 https://doi.org/10.1371/journal.pcbi.1003531.

Meisner, A., Jacquiod, S., Snoek, B.L., Ten Hooven, F.C., Van Der Putten, W.H., 2018. Drought legacy effects on the composition of soil fungal and prokaryote communities. Front. Microbiol. 9, 294. https://doi.org/10.3389/fmicb.2018.00294.

Newman, M.E.J., 2004. Analysis of weighted networks. Phys. Rev. E 70, 056131. https://doi.org/10.1103/PhysRevE.70.056131.

Olesen, J.M., Bascompte, J., Dupont, Y.L., Jordano, P., 2007. The modularity of pollination networks. Proc. Natl. Acad. Sci. U. S. A. 104, 19891–19896. https://doi.org/10.1073/pnas.0706375104.

Op De Beeck, M., Lievens, B., Busschaert, P., Declerck, S., Vangronsveld, J., Colpaert, J. V., 2014. Comparison and validation of some ITS primer pairs useful for fungal Metabarcoding studies. PLoS One 9, e97629. https://doi.org/10.1371/journal.pone.0097629.

Peng, G., Wu, J., 2016. Optimal network topology for structural robustness based on natural connectivity. Physica A Statis. Mech. Appl. 443, 212–220. https://doi.org/10.1016/j.physa.2015.09.023.

Perez-Lamarque, B., Krehenwinkel, H., Gillespie, R.G., Morlon, H., 2022. Limited evidence for microbial transmission in the phylosymbiosis between Hawaiian spiders and their microbiota. mSystems 7, e01104–e01121. https://doi.org/10.1128/msystems.01104-21.

Peterson, A.T., Soberón, J., Ramsey, J., Osorio-Olvera, L., 2020. Co-occurrence networks do not support identification of biotic interactions. Biodivers. Inform. 15, 1–10. https://doi.org/10.17161/bi.v15i1.9798.

Petrolli, R., Augusto Vieira, C., Jakalski, M., Bocayuva, M.F., Vallé, C., Cruz, E.D.S., Selosse, M., Martos, F., Kasuya, M.C.M., 2021. A fine-scale spatial analysis of fungal communities on tropical tree bark unveils the epiphytic rhizosphere in orchids. New Phytol. 231, 2002–2014. https://doi.org/10.1111/nph.17459.

Qiu, L., Zhang, Q., Zhu, H., Reich, P.B., Banerjee, S., van der Heijden, M.G.A., Sadowsky, M.J., Ishii, S., Jia, X., Shao, M., Liu, B., Jiao, H., Li, H., Wei, X., 2021. Erosion reduces soil microbial diversity, network complexity and multifunctionality. ISME J. 15, 2474–2489. https://doi.org/10.1038/s41396-021-00913-1.

Quast, C., Pruesse, E., Yilmaz, P., Gerken, J., Schweer, T., Yarza, P., Peplies, J., Glöckner, F.O., 2012. The SILVA ribosomal RNA gene database project: improved data processing and web-based tools. Nucleic Acids Res. 41, D590–D596. https://doi.org/10.1093/nar/gks1219.

Reimann, C., Filzmoser, P., Fabian, K., Hron, K., Birke, M., Demetriades, A., Dinelli, E., Ladenberger, A., 2012. The concept of compositional data analysis in practice — total major element concentrations in agricultural and grazing land soils of Europe. Sci. Total Environ. 426, 196–210. https://doi.org/10.1016/j.scitotenv.2012.02.032.

Rognes, T., Flouri, T., Nichols, B., Quince, C., Mahé, F., 2016. VSEARCH: a versatile open source tool for metagenomics. PeerJ 4, e2584. https://doi.org/10.7717/peerj.2584.

Röttjers, L., Faust, K., 2018. From hairballs to hypotheses–biological insights from microbial networks. FEMS Microbiol. Rev. 42, 761–780. https://doi.org/10.1093/femsre/fuy030.

Santolini, M., Barabási, A.-L., 2018. Predicting perturbation patterns from the topology of biological networks. Proc. Natl. Acad. Sci. U. S. A. 115 https://doi.org/10.1073/pnas.1720589115.

Shen, J., Wyness, A.J., Claire, M.W., Zerkle, A.L., 2021. Spatial variability of microbial communities and salt distributions across a latitudinal aridity gradient in the Atacama Desert. Microb. Ecol. 82, 442–458. https://doi.org/10.1007/s00248-020-01672-w.

Shi, S., Nuccio, E.E., Shi, Z.J., He, Z., Zhou, J., Firestone, M.K., 2016. The interconnected rhizosphere: high network complexity dominates rhizosphere assemblages. Ecol. Lett. 19, 926–936. https://doi.org/10.1111/ele.12630.

Stouffer, D.B., Bascompte, J., 2011. Compartmentalization increases food-web persistence. Proc. Natl. Acad. Sci. U. S. A. 108, 3648–3652. https://doi.org/10.1073/pnas.1014353108.

Sun, S., Li, S., Avera, B.N., Strahm, B.D., Badgley, B.D., 2017. Soil bacterial and fungal communities show distinct recovery patterns during forest ecosystem restoration. Appl. Environ. Microbiol. 83 https://doi.org/10.1128/AEM.00966-17 e00966-17.

Terrat, S., Dequiedt, S., Horrigue, W., Lelievre, M., Cruaud, C., Saby, N.P.A., Jolivet, C., Arrouays, D., Maron, P.-A., Ranjard, L., Chemidlin Prévost-Bouré, N., 2015. Improving soil bacterial taxa–area relationships assessment using DNA meta-barcoding. Heredity 114, 468–475. https://doi.org/10.1038/hdy.2014.91.

Tipton, L., Müller, C.L., Kurtz, Z.D., Huang, L., Kleerup, E., Morris, A., Bonneau, R., Ghedin, E., 2018. Fungi stabilize connectivity in the lung and skin microbial ecosystems. Microbiome 6, 12. https://doi.org/10.1186/s40168-017-0393-0.

Trivedi, P., Leach, J.E., Tringe, S.G., Sa, T., Singh, B.K., 2020. Plant–microbiome interactions: from community assembly to plant health. Nat. Rev. Microbiol. 18, 607–621. https://doi.org/10.1038/s41579-020-0412-1.

Turcotte, M.M., Corrin, M.S.C., Johnson, M.T.J., 2012. Adaptive evolution in ecological communities. PLoS Biol. 10, e1001332 https://doi.org/10.1371/journal.pbio.1001332.

Turley, N.E., Bell-Dereske, L., Evans, S.E., Brudvig, L.A., 2020. Agricultural land-use history and restoration impact soil microbial biodiversity. J. Appl. Ecol. 57, 852–863. https://doi.org/10.1111/1365-2664.13591.

Viruel, E., Fontana, C.A., Puglisi, E., Nasca, J.A., Banegas, N.R., Cocconcelli, P.S., 2022. Land-use change affects the diversity and functionality of soil bacterial communities in semi-arid Chaco region, Argentina. Appl. Soil Ecol. 172, 104362 https://doi.org/10.1016/j.apsoil.2021.104362.

Wagg, C., Schlaeppi, K., Banerjee, S., Kuramae, E.E., van der Heijden, M.G.A., 2019. Fungal-bacterial diversity and microbiome complexity predict ecosystem functioning. Nat. Commun. 10, 4841. https://doi.org/10.1038/s41467-019-12798-y.

Xu, Q., Vandenkoornhuyse, P., Li, L., Guo, J., Zhu, C., Guo, S., Ling, N., Shen, Q., 2022. Microbial generalists and specialists differently contribute to the community diversity in farmland soils. J. Adv. Res. 40, 17–27. https://doi.org/10.1016/j.jare.2021.12.003.

Yu, Y., Shi, Y., Li, M., Wang, C., Zhang, L., Sun, Z., Lei, B., Miao, Y., Wang, W., Liu, B., Zheng, J., Chu, H., Han, S., 2022. Land-use type strongly affects soil microbial community assembly process and inter-kingdom co-occurrence pattern in a floodplain ecosystem. Appl. Soil Ecol. 179, 104574 https://doi.org/10.1016/j.apsoil.2022.104574.

Yuan, M.M., Guo, X., Wu, Linwei, Zhang, Y., Xiao, N., Ning, D., Shi, Z., Zhou, X., Wu, Liyou, Yang, Y., Tiedje, J.M., Zhou, J., 2021. Climate warming enhances microbial network complexity and stability. Nat. Clim. Chang. 11, 343–348. https://doi.org/10.1038/s41558-021-00989-9.